Supplemental Figures

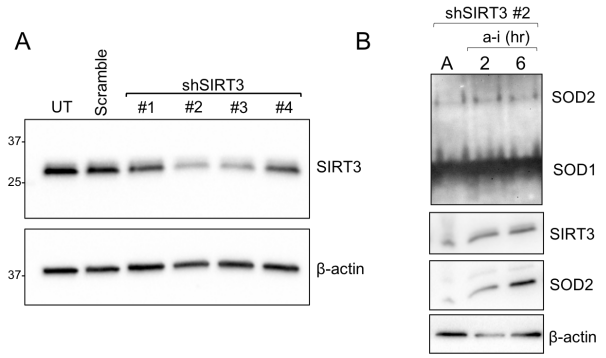

Supplemental Figure 1: A SIRT3 protein expression knock-down following transient transfection of four shRNAs targeting SIRT3. shRNAs #2 and #3 were chosen for the establishment of OVCA433 stable knock-down cells. **B.** SIRT3 knock-down by shRNA construct #2 inhibits the a-i induced SOD2 activity within 2 h of matrix detachment. SOD2 activity was assessed by zymography in attached (A) OVCA433 cells and cells cultured for 2 or 6 h in anchorage-independence (a-i).

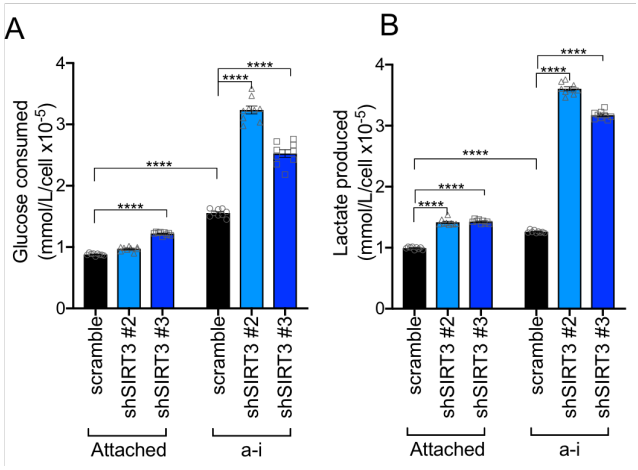

Supplemental Figure 2: Media glucose (**A**) and lactate (**B**) levels were measured using the YSI biochemical analyzer and expressed as Glucose consumed and lactate produced by correcting for media glucose and lactate levels respectively, and expressed relative to cell numbers (n=9; one-way ANOVA P=0.01, Tukey's multiple comparisons test ****P<0.0001).

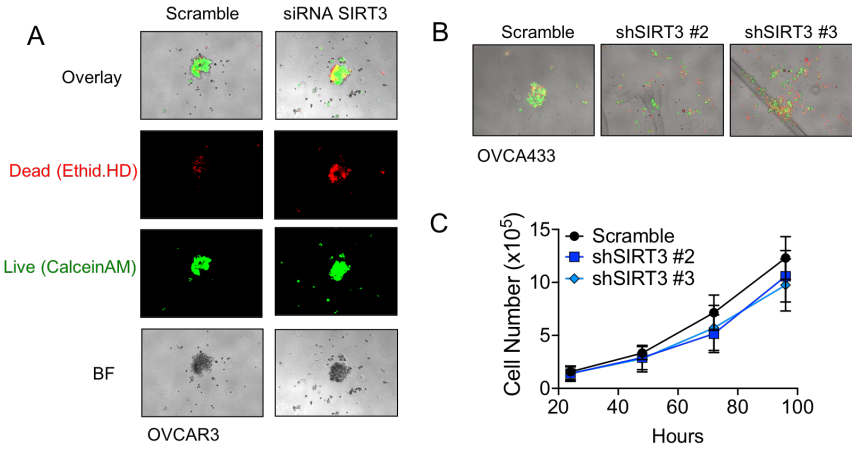

Supplemental Figure 3: A. SIRT3 knock-down via siRNA delivery increases the dead cell fraction of OVCAR3 cells cultured as spheroid aggregates for 72 h in ULA plates. Cells were stained for live and dead cells using Ethidium HomoDimer and Calcein AM, respectively. **B.** Stable SIRT3 knock-down via shRNA inhibits rapid aggregation of OVCA433 in anchorage-independent cell culture conditions. 1,000 cells were plated per well in 96 well ULA culture plates and live dead staining carried out 6 hours after seeding. **C.** SIRT3 knock-down does not significantly affect OVCA433 cell proliferation in attached conditions (n=3).

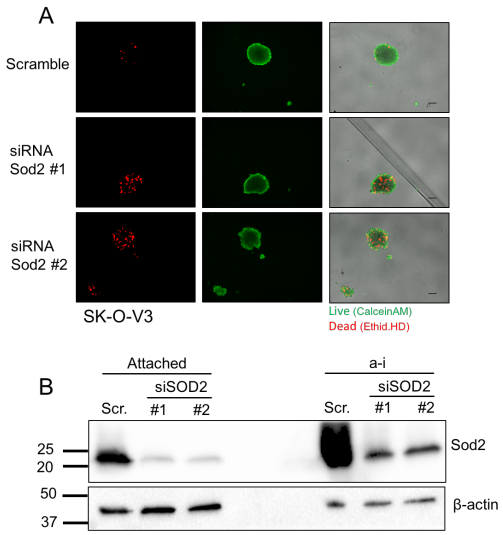

Supplemental Figure 4: A. SOD2 knock-down decreases cell viability in SK-OV-3 cells cultured in anchorage-independence for 72 h. Cells were stained for live and dead cells using Ethidium HomoDimer and Calcein AM, respectively. **B.** Western blot analysis of Sod2 expression in SK-OV-3 cells following siRNA mediated knock-down.

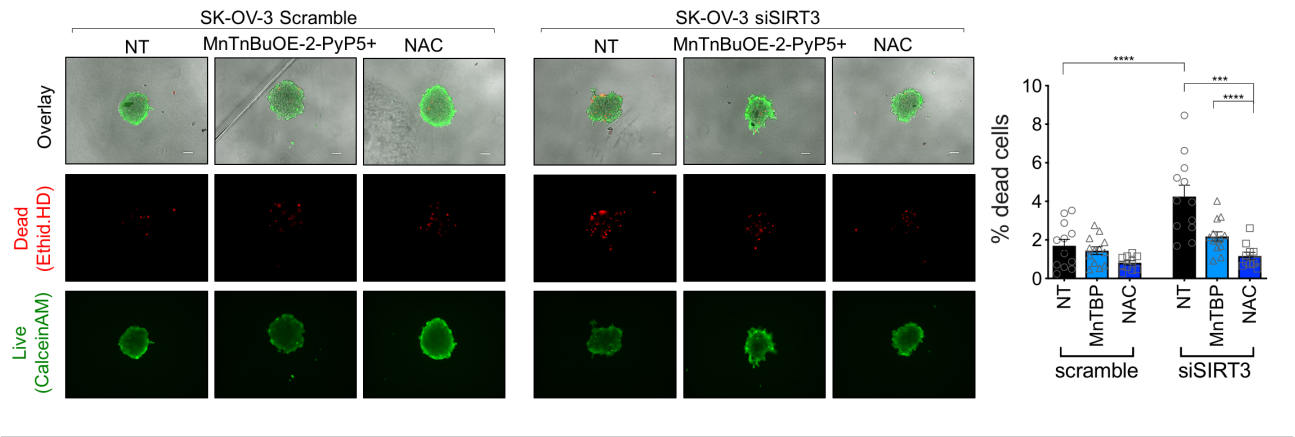

Supplemental Figure 5: Treatment of cells with 10μM MnTBAP or 2mM NAC rescues SK-OV-3 cell viability.

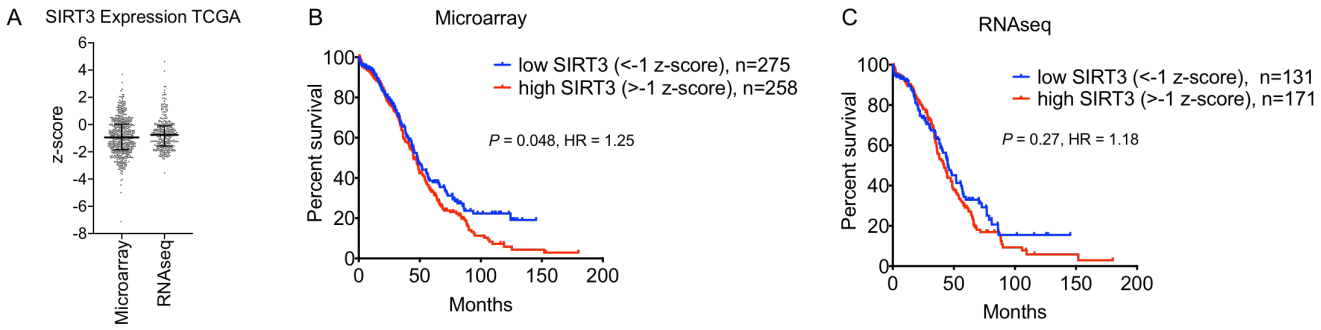

Supplemental Figure 6: A. Spread of SIRT3 expression in TCGA serous ovarian adenocarcinoma samples subjected to Agilent micro-array (n=533) and RNAseq (n=303) analysis (median with interquartile range indicated). **B & C.** Kaplan Meier curves of overall survival of samples subjected to Microarray analysis (**B**), and RNA seq analysis (**C**). Samples with SIRT3 expression z-score <-1 were compared to those with z score >-1. (Log-rank Mantel-Cox test).

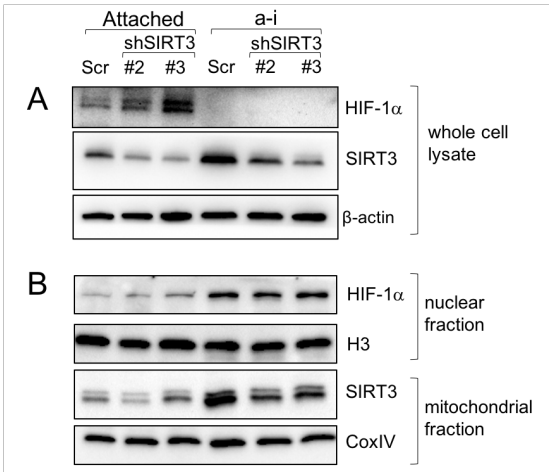

Supplemental Figure 7: SIRT3 knock-down does not affect HIF-1α levels in anchorage-independent conditions (a-i). **A.** SIRT3 knock-down increases total HIF-1α levels in attached conditions only. (Representative blot shown - same lysates as Figure 2F). **B.** HIF-1α nuclear localization is enhanced in a-i compared to attached conditons. SIRT3 knock-down does not affect HIF-1α nuclear localization in a-i.

Supplemental Methods

Optical Redox Ratio imaging. Anchorage-independent spheroids were imaged using the Nikon A1 MP+ Multi-Photon Microscope system (Nikon Instruments, New York) to assess endogenous fluorescence signals produced by NAD(P)H and FAD, using a mode-locked femto-second Spectra-Physics InSight DS femtosecond single-box laser system with automated dispersion compensation tunable between 680-1300 nm (Spectra-Physics, Mountain View, CA) and Nikon scan head coupled with Nikon upright microscope system (Nikon Instruments, New York). The laser output was attenuated using AOTF and the average power was consistently maintained below the damage threshold of the samples. The laser beam tuned to 1000 nm was then focused on the specimen through a high numerical aperture, low magnification, long working distance, dipping objective, CFI75 Apo Water 25X/1.1 LWD 2.0mm WD, and backscattered emissions collected through the same objective lens. Nikon Element Software was used for the image acquisition. In the reflection mode, non-descanned high-sensitivity GaAsP detectors were used for very efficient signal detection. A 750 nm Dichroic was used to prevent the scattered IR laser radiation from reaching the detector and a 460 nm long pass dichroic beam splitter (460 DCLP, Chroma Technology, USA) was used to collect NAD(P)H signal below 460 nm, a 560 nm long pass dichroic beam splitter (560 DCLP, Chroma Technology, USA) and a 660 nm long pass dichroic beam splitter (660 DCLP, Chroma Technology, USA) were used to collect FAD signal above 560 and below 660 nm. Spectral measurements to confirm the presence of NAD(P)H and FAD signals were also performed using 32-channel Nikon Spectral Detector integrated with Nikon A1 MP+ Multi-Photon Microscope system. For 3D image data set acquisition, the multiphoton excitation beam tuned to 1000 nm was first focused at the maximum signal intensity focal position within the spheroid sample and the appropriate detector levels were then selected to obtain the voxel intensities within range of 0-4095 (12-bit images) using a color gradient function. Later on, the beginning and end of the 3D stack (i.e. the top and the bottom optical sections) were set based on the signal level degradation. A series of 2D Images for a selected 3D stack volume were then acquired at 512 X 512 pixels. The 3D stack images with optical section thickness (z-axis) of approximately 2.0 μm were captured with voxel size of 0.5 X 0.5 X

2μm. For each spheroid volume reported, z-section images were compiled and the 3D image restoration performed using VOLOCITY (Perkin Elmar, UK). The volume estimation was performed on the 3D image data sets recorded from at least 3 spheroids. A noise removal filter was applied, and the lower threshold level in the histogram set to exclude all possible background voxel values. Sum of all voxels intensities above this threshold level was determined to be total NAD(P)H and FAD signals. The optical redox ratio was calculated from mean voxel intensity values using the equation, FAD/(FAD+NAD(P)H).

TCGA analysis. Agilent micro-array (n=533) and RNAseq (n=303) expression data from high grade serous adenocarcinomas were obtained from the cancer genome atlas (TCGA), using the cBioPortal interface (cBioportal.org; z-score spread of SIRT3 expression) [1]. Overall survival was plotted using GraphPad Prism software and statistical differences determined using log rank test (Mantel-Cox).

Supplemental Reference:

1 Cerami E, Gao J, Dogrusoz U, Gross BE, Sumer SO, Aksoy BA *et al*. The cBio cancer genomics portal: an open platform for exploring multidimensional cancer genomics data. Cancer Discov 2012; 2: 401-404.